Available online at www.sciencedirect.com

SciVerse ScienceDirect

Ceramics International 39 (2013) S65–S68

CERAMICS INTERNATIONAL

www.elsevier.com/locate/ceramint

Densification behaviour and two stage master sintering curve in lithium sodium niobate ceramics

Supratim Mitra, Ajit R Kulkarni*, Om Prakash

Department of Metallurgical Engineering and Materials Science, Indian Institute of Technology Bombay, Mumbai 400076, India

Available online 16 October 2012

Abstract

The Master Sintering Curve (MSC) has received much attention in recent years due to its ability to predict sintering behaviour of a given powder and green body process regardless of its thermal history. In this paper MSC, based on the combined stage sintering model is constructed for one of the most important lead-free piezoelectric *viz*. lithium sodium niobate, $Na_{1-x}Li_xNbO_3$ ($x=0.12$, LNN-12), ceramic using shrinkage data. The present study has been carried out to understand and control the densification behaviour during pressureless sintering. Two distinct stages of densification have been observed en route to the upper limit to sintering temperature. The activation energies of densification for the two temperature ranges *viz*. 800–1150 °C and 1150–1300°C were found to be 365 kJ/mol and 2530 kJ/mol, respectively, through the construction of MSC. The MSC should be useful in predicting the densification behaviour and the final density and for designing a reproducible fabrication schedule for the LNN-12 ceramics.

Keywords: A. Sintering; C. Diffusion; D. Niobates; Master sintering curve

1. Introduction

In recent years, demand for the new, lead-free piezoelectric materials for technological applications has increased because of environmental concerns. Among the many lead-free piezoelectric ceramic systems investigated, alkali niobate piezoelectric ceramics have been found to be attractive due to their excellent piezoelectric properties (*viz.* piezoelectric coefficient, $300 < d_{33} < 400$ pC/N; electromechanical coupling constant, $0.4 < k_p < 0.6$; mechanical quality factor, $200 < Q_m < 700$) and high Curie temperature ($T_c \sim 400$ °C). It has been reported that lithium sodium niobate, $Na_{1-x}Li_xNbO_3$, a promising system for high frequency applications, offers a relatively high electromechanical coupling, $k_p \sim 0.4$, and significant mechanical quality factor, $Q_m \sim 755$, at its morphotropic phase boundary (MPB) composition, $x=0.12$ ($Li_{0.12}Na_{0.88}$) NbO_3 (LNN-12) [1]. These property parameters are, however, found to be strongly dependent on the materials final density, synthesis technique followed, and sintering parameters [2,3]. The process parameters which influence sintering the most are: temperature, holding time, initial particle size, green density and bulk composition [4,5]. The parameters such as holding time (t) and temperature (T) of sintering are decided either through the preliminary exploratory runs or the ceramic phase diagram or both. Further, any changes to these parameters may cause undesired density, shape distortion, warping, development of cracks and microstructural damages in the final product. Therefore, there is a need to predict the sintering behaviour *ab initio*, from the experimental data, to have a final product with desired density and microstructure (and also with less number of sample rejections). It is reported that the theory of Master Sintering Curve (MSC) provides a powerful tool to predict the densification behaviour during sintering under different thermal profiles for a chosen powder processing method [6,7]. For a given powder and green body, the instantaneous relationship between activation energy of sintering, Q and relative physical density (ρ) could be established through the construction of an MSC [6,7]. Considering, only one diffusion mechanism (either volume diffusion or grain boundary diffusion) and microstructure is only density (ρ) dependent, the MSC can be

*Corresponding author. Tel.: +91 22 2576 7636; fax: +91 22 2572 3480.
E-mail address: ajit.kulkarni@iitb.ac.in (A. R Kulkarni).

0272-8842/$ - see front matter © 2012 Elsevier Ltd and Techna Group S.r.l. All rights reserved.
http://dx.doi.org/10.1016/j.ceramint.2012.10.036

constructed by the equation as given by,

$$\Phi(\rho) = \Theta(t, T(t)) \equiv \int_0^t \frac{1}{T} exp\left(-\frac{Q}{RT}\right) dt \quad (1)$$

where, Q is the activation energy of sintering, T is the absolute temperature, t is the time, R is the gas constant and $\Phi(\rho)$ is related to the microstructural evolution and $\Theta(t,\ T(t))$ is a function of the thermal history.

The model of MSC, in the recent past, has been applied successfully to many of the ceramic oxides such as ThO_2 [8], ZnO [6,9], Al_2O_3 [6], Al_2O_3+5% ZrO_2 [6], 3Y-TZP [10], 8YSZ and Al_2O_3 doped 8YSZ [11]. However, little attention has been paid to the studies on the formulation of MSC for lead-free alkali niobate ceramics. In the present work, from the non-isothermal sintering experiment(s), an MSC is constructed for the $Li_{0.12}Na_{0.88}NbO_3$ (LNN-12) composition to predict the densification behaviour and also to estimate the activation energy of sintering.

2. Experimental

All the LNN-12 samples in this study were prepared from the reagent-grade Nb_2O_5, Na_2CO_3 (both 99.5% pure, Loba Chemie, India) and Li_2CO_3 (99.0% pure, Merck, India). These were mixed in the desired stoichiometry of $Na_{1-x}Li_xNbO_3$ (x=0.12), and wet ball milled in alcohol to obtain proper mixing and a surface-active fine powder. After solid state reacted at 900 °C for 4 h in air to achieve single phase powder, the reacted powder was reground and average volume particle size distribution was measured using laser diffraction particle size analyzer (Beckman Coulter, LS 13 320). The powder was then pressed uniaxially into cylindrical pellets of 10 mm diameter and 14.5 mm length using pressure of 450 MPa. Linear shrinkage (from room temperature to 1300°C) of the cylindrical pellet was recorded in the axial direction using a 2016STD (Orton, USA) push rod type dilatometer, calibrated using standard alumina sample (Orton, USA) under heating rate 10 °Cmin^{-1}. Both, the temperature and the length of the sample were recorded continuously with the help of a thermocouple and a linear voltage differential transducer (LVDT) respectively. The phase formation was confirmed from the powder X-Ray Diffraction (XRD) data and theoretical density (TD) was calculated from the calculated lattice parameters of the LNN-12 sample using Rietveld refinement technique as implemented in the computer programme package FullProf 2000 [12].

3. Results and discussion

3.1. Powder characterization

For the samples, clean single phase (orthorhombic) polycrystalline LNN-12 formation was confirmed from the XRD pattern wherein all the peak positions matched well with the JCPDS#033 1270 [13]. Rietveld refinements of the XRD data were carried out by selecting the space group

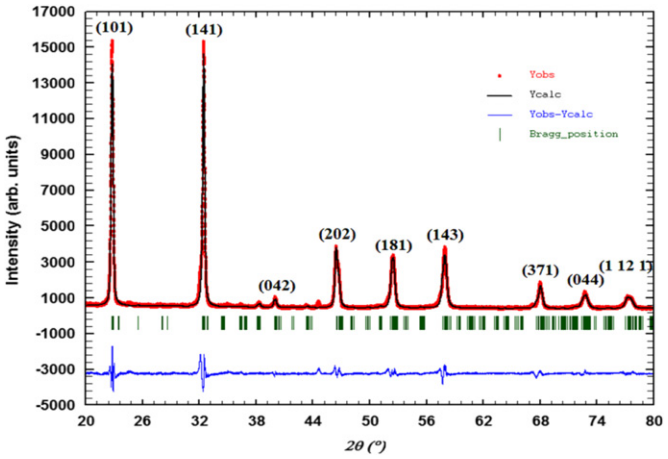

Fig. 1. (Colour online) Powder XRD pattern of a nominal LNN-12 sample in the space group $Pc2_1b$. The dots represent the observed data points and the solid lines their Rietveld fit.

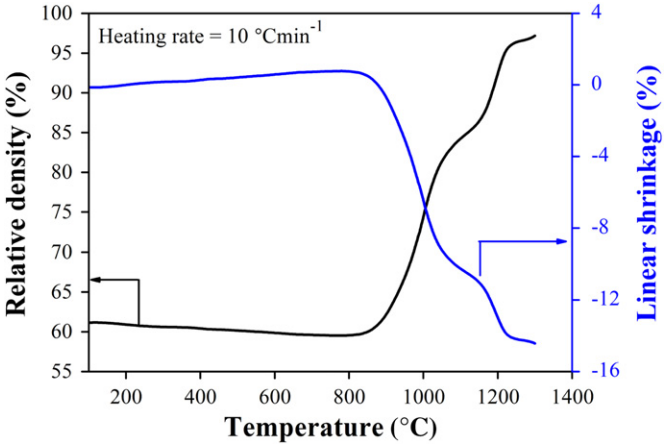

Fig. 2. (Colour online) Relative density (%) and normalized linear shrinkage profile of LNN-12 green compacted sample over a temperature range. The sintering of the sample commences above 800 °C.

$Pc2_1b$ (29) [14]. Fig. 1 depicts the observed, calculated and different XRD profiles of the LNN-12 sample after the final cycle of refinement.The refined unit cell parameters, unit cell volume are found to be a=5.5083(Å), b=15.5406 (Å), c=5.5414 (Å), V_{cell}=474.36 (Å^3) respectively. Theoretical density (TD)=4.53 g/cc was calculated from the above refined lattice parameters. Average particle size $\overline{d} \sim 0.69$ μm was measured using laser diffraction particle size analyzer.

3.2. Densification

Both, the relative density (%) and normalized linear shrinkage ($\Delta L/L_0$) versus temperature (T°C) curves for a green compacted LNN-12 sample, subjected to a heating rate of 10 °C min^{-1}, from room temperature to 1300 °C, in air, is shown in Fig. 2. The shrinkage (ΔL) values were converted into relative density by assuming isotropic

shrinkage during sintering using the relation,

$$\text{Relative density}\ (\%) = \left(1-\frac{\Delta L}{L_0}\right)^{-3}\frac{\rho_0}{\rho}100 \qquad (2)$$

where L_0 is the initial length, ρ (=4.53 g/cc) is the theoretical density, and ρ_0 (=0.609ρ) is the measured green density of the compacted pellet. It can be seen from Fig. 2 that a slight thermal expansion occurs up to ~890 °C, while at temperatures >890 °C sample shrinkage commences with a steep shrinkage at ~1000 °C. On increasing the sintering temperature further, another weak shrinkage shoulder is observed at ~1195 °C reaching density ~85%; the curve plateaus out at ~1225 °C reaching a final density ~97%. In ideal case both densification and grain growth should proceed together, but in the case of LNN-12 ceramic a lag between these two processes has been found which leads to two distinct steps in the densification curve. The presence of soft agglomerates in the fine phase powder LNN-12, and so the inhomogeneous distribution of porosity in the green compacted sample influences the mobility of grainboundary during sintering [15].

3.3. Construction of master sintering curve (MSC)

In view of the discussion in the preceding section, the activation energies of densification in the two discrete stages were determined separately via the construction of MSC as there is freedom in constructing MSC over several consecutive stages, based on either the temperature [16] or the density range [17,18]. Conventionally, MSC is constructed using shrinkage data from dilatometer experiments if the activation energy, Q, is known and as a simple approach, constant heating rate experiments are usually performed to estimate the Q-value. For this, a particular value of activation energy, Q is chosen and ρ-$\Theta(t,T(t))$ trajectory is constructed for different heating rates. The sets of data are then fitted by a modified sigmoid function [19] *viz*,

$$\rho = \rho_0 + \frac{a}{\left\{1+exp\left(-\frac{log(\Theta)-log(\Theta_0)}{b}\right)\right\}^c} \qquad (3)$$

where a, b and c are the appropriately selected constants, $log(\Theta_0)$ is the abscissa coordinate of the reflection pointof the curve, ρ_0 is the green density, to determine the exact form of the sigmoid curve and a better fit to theMSC. The Q-value that yields the minimum mean residual square (MRS) that obtained from the fitting of sigmoid function is selected for the construction of MSC. This is, however, a time consuming and tedious process and sometimes fails to reflect the physical reality. Therefore, to overcome this problem we have adopted a computer programme, developed in Visual Basic for Application (VBA) by Chen et al. [19] that facilitates to choose more precisely the activation energy for the construction of MSC. The programme gives the best fit results for the calculation of Q-value. Hence, the approach of having a single heating rate for the green

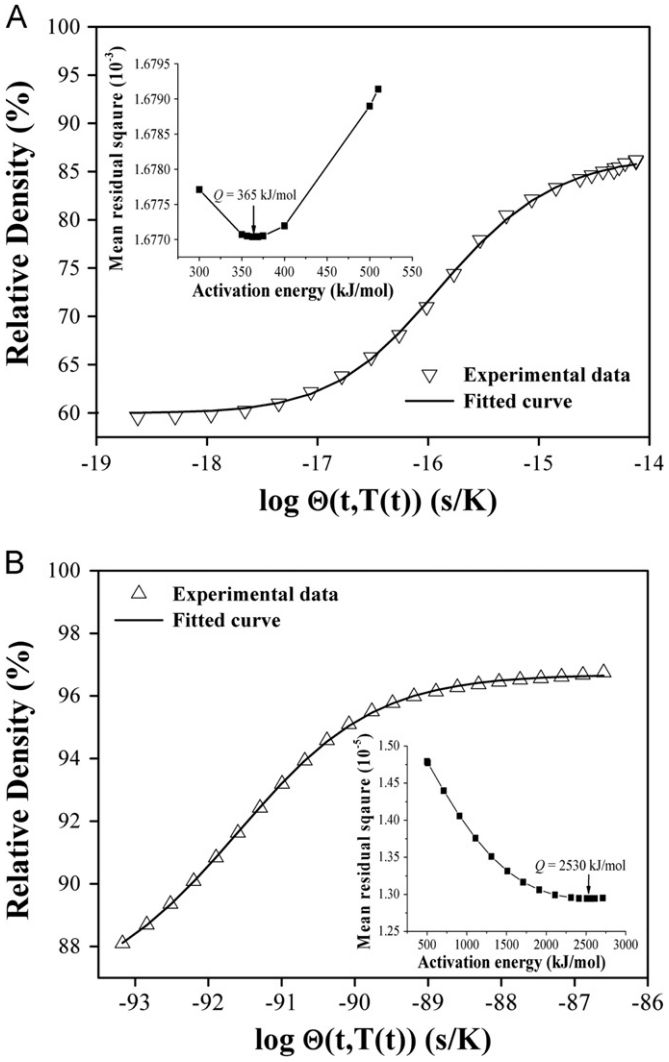

Fig. 3. For the LNN-12 ceramic sample, construction of (A) MSC for the temperature range 800–1150 °C; the inset shows the minimum of mean residual square at Q=365 kJ/mol and (B) MSC for the temperature range 1150–1300 °C; the inset shows the minimum of mean residual square at Q=2530 kJ/mol.

LNN-12 sample was experimentally simple and sufficient to have the desired data. A moderate heating rate of 10 °C min^{-1} was, therefore, chosen to minimize the contribution from surface diffusion at low temperatures [20]. The time of surface diffusion regime is comparatively small unless one uses extremely low constant heating rates. The MSCs for LNN-12 ceramic were constructed for the temperature ranges 800–1150 °C and 1150–1300 °C by using input data points (temperature (°C), time (s), relative density (%)) obtained from the dilatometer experiment for each of the temperature range. Fig. 3 shows the constructed MSCs realized through the best fitted ρ-$\Theta(t, T(t))$ curve (see Eq. (3)); and the inset figures show the MRS-values for the various activation energies. The activation energy with minimum MRS value has been selected to construct MSC. For the initial temperature range, activation energy of 365 kJ/mol is found, and is believed to a

lesser extent to be the mode of a grain boundary diffusion; whereas, for the final temperature range, activation energy of 2530 kJ/mol was obtained; the corresponding dominant diffusion/sintering path way could not be figured out. It is, therefore viewed that, during the last part of sintering/densification, more than one diffusion mechanism may be operative.

4. Conclusions

For LNN-12 composition, the activation energies for a two step process of densification were determined with the help of MSC. The MSC was successfully constructed for the LNN-12 ceramic. An appropriate representation of densification behaviour was possible by applying two stage MSC approach for the two different temperature ranges. The MSC should be useful to the ceramic industries to predict and control the densification evolution at a given sintering/thermal profile for the realistic desired density of their sinterable products.

Acknowledgements

Thanks are due to Prof. Mao-Hua Teng for providing the computer programme of master sintering curve model to facilitate predicting accurately the sintering results.

References

[1] R.M. Henson, R.R. Zeyfang, K.V. Kiehl, Dielectric and electromechanical properties of (Li,Na)NbO_3 ceramics, Journal of the American Ceramic Society 60 (1977) 15–27.
[2] B. Hardiman, R.M. Henson, C.P. Reeves, R.R Zeyfang, Hot pressing of sodium lithium niobate ceramics with pervoskite-type structures, Ferroelectrics 12 (1976) 157–159.
[3] Q. Chen, Z. Peng, H. Liu, D. Xiao, J. Zhu, J. Zhu, The crystalline structure and phase-transitional behavior of $(Li_{0.12}Na_{0.88})(Nb_{1-x\%}Sb_{x\%})O_3$ lead-free piezoelectric ceramics with high Qm, Journal of the American Ceramic Society 93 (2010) 2788–2794.
[4] H. Matzke, Atomic mechanisms of mass transport in ceramic nuclear fuel materials, Journal of the Chemical Society-Faraday Transactions 86 (1990) 1243–1256.
[5] C.R.A. Catlow, Recent problems and progress in the study of UO_2 and mixed UO_2–PuO_2, Journal of the Chemical Society-Faraday Transactions 2 (83) (1987) 1065–1072.
[6] H. Su, D.L. Johnson, Master sintering curve: a practical approach to sintering, Journal of the American Ceramic Society 79 (1996) 3211–3217.
[7] S. Hunghai, D.L. Johnson, Practical approach to sintering, American Ceramic Society Bulletin 76 (1997) 72–76.
[8] T.R.G. Kutty, K.B. Khan, P.V. Hegde, J. Banerjee, A.K. Sengupta, S. Majumdar, H.S. Kamath, Development of a master sintering curve for ThO_2, Journal of Nuclear Materials 327 (2004) 211–219.
[9] K.G. Ewsuk, D.T. Ellerby, C.B. DiAntonio, Analysis of nanocrystalline and microcrystalline ZnO sintering using master sintering curves, Journal of the American Ceramic Society 89 (2006) 2003–2009.
[10] M. Mazaheri, A. Simchi, M. Dourandish, F. Golestani-Fard, Master sintering curves of a nanoscale 3Y-TZP powder compacts, Ceramics International 35 (2009) 547–554.
[11] X. Song, J. Lu, Two-stage master sintering curve approach to sintering kinetics of undoped and Al_2O_3-doped 8 mol% yittria-stabilized cubic zirconia, Journal of the American Ceramic Society 94 (2011) 1053–1059.
[12] J. Rodriguez-Carvajal, FullProf 2000: A Rietveld Refinement and Pattern Matching Analysis Program (Version: July 2001), Laboratoire Léon Brillouin (CEA-CNRS), France.
[13] JCPDS-International Centre for Diffraction, Data nos. 033-1270.
[14] Inorganic Crystal Structure Database, ICSD Database Code 38314, 1984.
[15] A.S. Edelstein, R.C. Cammarata, Nanomaterials: Synthesis, Properties and Applications, Institute of Physics Publishing, London, UK, 1998.
[16] D.C. Blaine, S.J. Park, R.M. German, Master sintering curve for a two-phase material, in: Proceedings of the 4th International Conference on Science, Technology and Application of Sintering 2005, Grenoble, France, 2005pp. 264–267.
[17] S. Kiani, J. Pan, J.A. Yeomans, A new scheme of finding the master sintering curve, Journal of the American Ceramic Society 89 (2006) 3393–3396.
[18] D.C. Blaine, S.J. Park, R.M. German, Linearization of master sintering curve, Journal of the American Ceramic Society 92 (2009) 1403–1409.
[19] M.H. Teng, Y.C. Lai, Y.T. Chen, A computer program of master sintering curve model to accurately predict sintering results, Western Pacific Earth Sciences 2 (2002) 171–180.
[20] T.R.G. Kutty, K.B. Khan, P.V. Hegde, A.K. Sengupta, S. Majumdar, H.S. Kamath, Determination of activation energy of sintering of ThO_2–U_3O_8 pellets using the master sintering curve approach, Science of Sintering 35 (2003) 125–132.